Precision Engineering 41 (2015) 63–67

Contents lists available at ScienceDirect

Precision Engineering

journal homepage: www.elsevier.com/locate/precision

Verification of the positioning accuracy of industrial coordinate measuring machine using optical-comb pulsed interferometer with a rough metal ball target

Wiroj Sudatham[a,*], Hirokazu Matsumoto[a], Satoru Takahashi[b], Kiyoshi Takamasu[a]

[a] Department of Precision Engineering, The University of Tokyo, Hongko 7-3-1, Bunkyo-ku, Tokyo 113-8656, Japan
[b] Research Center for Advanced Science and Technology, The University of Tokyo, Komaba 4-6-1, Meguro, Tokyo 153-8904, Japan

ARTICLE INFO

Article history:
Received 29 October 2014
Received in revised form
21 December 2014
Accepted 19 January 2015
Available online 7 February 2015

Keywords:
Optical comb
Pulsed interferometer
Length measurement
Coordinate measuring machine
CMM

ABSTRACT

An optical-comb pulsed interferometer was developed for the positioning measurements of the industrial coordinate measuring machine (CMM); a rough metal ball was used as the target of the single-mode optical fiber interferometer. The measurement system is connected through a single-mode fiber more than 100 m long. It is used to connect a laser source from the 10th floor of a building to the proposed measuring system inside a CMM room in the basement of the building. The repetition frequency of a general optical comb is transferred to 1 GHz by an optical fiber-type Fabry–Pérot etalon. Then, a compact absolute position-measuring system is realized for practical non-contact use with a high accuracy of measurement. The measurement uncertainty is approximately 0.6 μm with a confidence level of 95%.

1. Introduction

A coordinate measuring machine (CMM) is defined by ISO 10360-1 as a measuring system with the means to move a probing system and the capability of determining spatial coordinates on a workpiece surface [1]. CMMs are widely used to measure the three-dimensional sizes, forms, and positions of manufactured parts. However, CMM measurement inaccuracy occurs when there is an error in the relative position between the measured points and the probing points. The errors affecting a CMM have a systematic and a random component. They also directly influence the quality of production inspection [2]. Therefore, CMMs must be calibrated on installation and verified periodically during their operation. The standards and guidelines for CMM verification are based on sampling the length-measurement capability of a CMM to decide whether its performance conforms to the specification [3,4]. Many methods and artifacts are developed to verify CMMs [2–10]. Most standards prefer to use end standards such as a series of gauge blocks, a step gauge, and a ball plate or laser interferometer. However, there is no one perfect method for CMMs, mainly because of the complicated constructions and the three-dimensional positions of many measured points that are necessary in coordinate metrology. In addition, the range of positioning verification is limited by the length of end standards [11,12]. Although a continuous-wave (cw) laser interferometer can measure for the long length, the measuring path cannot be interrupted during the measurement period because it is operated by a cw laser and interference fringe counting method.

Recently, an optical frequency comb has been considered as a useful tool for dimensional metrology, because of their high frequency-stability and direct traceability to SI unit [13]. Several methods for length measurement with an optical frequency comb have been proposed [14–17]. This paper proposes a new technique for the verification of the positioning accuracy of CMMs using an optical-comb pulsed interferometer. A rough metal ball is used as the target of a single-mode fiber interferometer. Because the sphere ball provides 3D targets, the measuring system can be constructed at any location on the surface of a CMM. In addition, the proposed measuring system can be installed on more than one system to measure many positions at the same time with a target as shown in Fig. 1.

A single-mode optical fiber more than 100 m long is used to connect a laser source from a 10th floor of a building to the proposed measuring system inside a CMM room in the basement of the building. The repetition frequency of a general optical comb is transferred to 1 GHz by an optical fiber-type Fabry–Pérot etalon.

* Corresponding author. Tel.: +81 3 5841 6472; fax: +81 3 5841 6472.
E-mail address: wiroj@nanolab.t.u-tokyo.ac.jp (W. Sudatham).

http://dx.doi.org/10.1016/j.precisioneng.2015.01.007
0141-6359/

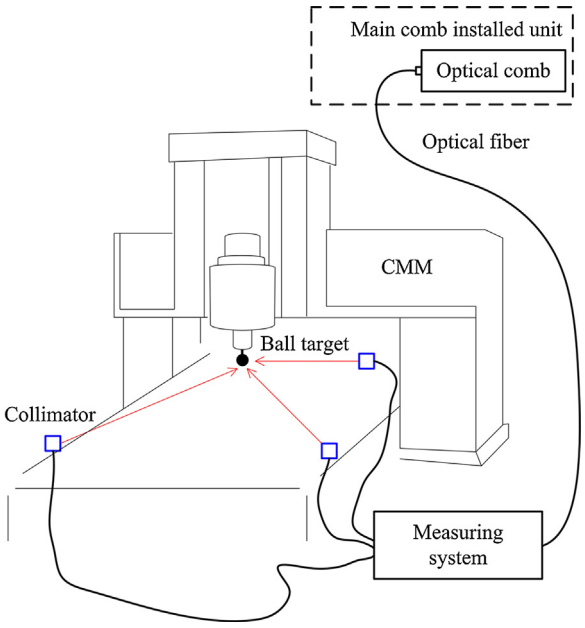

Fig. 1. The concept idea of CMM verification using an optical-comb pulsed interferometer with a rough metal ball target.

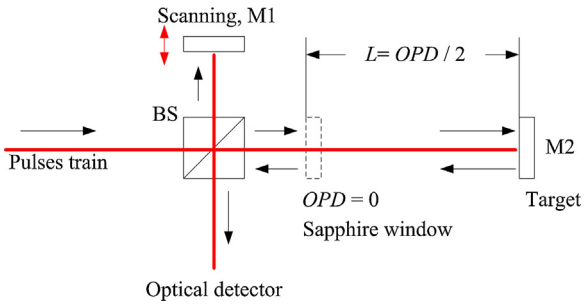

Fig. 2. Principle of an optical-comb pulsed interferometer.

Then, a compact absolute position-measuring system is established based on a single-mode fiber interferometer; a rough metal ball is used as the target because the alignment of the laser beam is easy. The conversion of the time scale, which is presented by envelope interference fringes, to the length scale is measured. The effect of the surface roughness of the target is also examined. The position errors of a moving bridge-type CMM were measured by the proposed measuring system paired with a commercial cw laser interferometer. Finally, the measurement uncertainty is also evaluated. The uncertainty of the measurement is approximately 0.6 μm with a confidence level of 95%. This technique provides enough accuracy for industrial CMMs.

2. Optical-comb pulsed interferometer

Mode-locked lasers generate ultrashort optical pulses by establishing a fixed-phase relationship across broad spectrum of frequencies. The spectrum of each pulse train is separated by the repetition rate of an optical comb, and the series of spectrum lines is called an optical frequency comb. In the time domain, the pulse train is emitted at the same time by a mode-locked laser [13]. The pulsed interferometer remains the principle of an unbalanced-arm Michelson interferometer where an optical comb is a laser source. As shown in Fig. 2, an optical comb generates a pulse train. Laser pulses are divided into two beams by an optical beam splitter (BS). One beam is reflected on a scanning mirror (M1), while the other

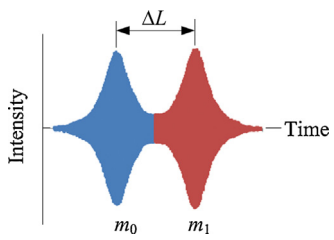

Fig. 3. Two interference fringes of an optical-comb pulsed interferometer; m_0 and m_1 are the fringe order at the reference position and the target position, respectively.

is transmitted through a sapphire window (reference position) to the target mirror (M2).

Subsequently, the reflected light pulses from a scanning mirror (M1) are recombined with the returned light pulses from a sapphire window and a target mirror (M2) to produce interference fringes when the optical path difference (*OPD*) between two arms follows Eq. (1) [14].

$$OPD = \frac{mc}{nf_{rep}} \tag{1}$$

where m is an integer, c is the speed of light in the vacuum, n is the refractive index of air, and f_{rep} is the repetition frequency.

Normally, two interference fringes will overlap when an optical-comb pulsed interferometer exactly satisfies the condition of Eq. (1). In practical use, the envelope peak of the interference fringes will be separated if displacement is provided (ΔL). The result is illustrated in Fig. 3.

Therefore, the position/length under measurement is determined by Eq. (2).

$$L = \frac{OPD}{2} + \Delta L \tag{2}$$

In application, two envelope interference fringes in Fig. 3 are presented in the time domain. The first fringe comes from the reference position when the *OPD* is zero ($m_0 = 0$), and the second fringe comes from the target when the *OPD* is around 300 mm ($m_1 = 1$). Therefore, the conversion of the time scale to the length scale of the peak-to-peak measurement of the envelope interference fringes must be measured because it relates to the speed of the scanning-fringe device. Moreover, the position/length under measurement must be corrected for the group refractive index of air due to changes in environmental conditions [18].

3. Experiments and results

3.1. Time scale and length scale measurement

The relationship between the time scale and the length scale measurement is required because the peak-to-peak of the envelope interference fringes shown in Fig. 3 is presented in the time domain. The measurement setup diagram to determine this relation is shown in Fig. 4.

A laser source (an optical comb C-Fiber Femtosecond Laser, Menlo Systems) generates a short pulse train with a repetition frequency of 100 MHz and a central wavelength of 1560 nm. The repetition rate was modified by a Fabry–Pérot fiber etalon. An optical fiber-type etalon was prepared from a special-cut length of a single-mode optical fiber (SMF-28). Both ends of the fiber are FC connectors (fiber-optic connector) whose surfaces are coated with 93% reflectivity to generate a 1-GHz FSR (free spectral range). The stability of repetition frequency after passing through a Fabry–Pérot fiber etalon was observed by a universal counter (SC-7206, Iwatsu). It was performed at an order of 10^{-9} over 2 h [16]. Subsequently, the laser beam was amplified by an optical amplifier.

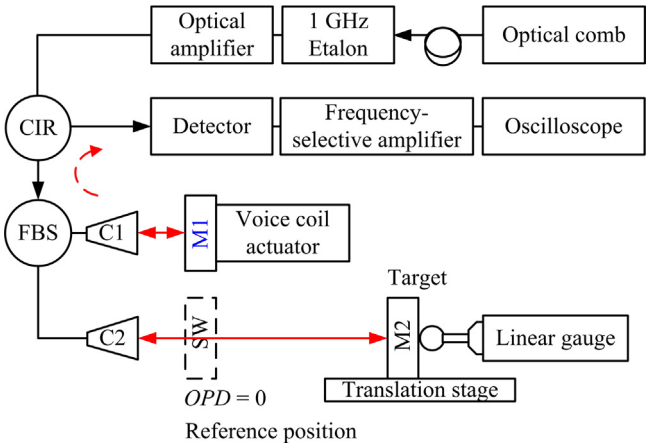

Fig. 4. Measurement setup diagram of the relationship between time scale and length scale measurement; CIR is optical fiber circulator, FBS is fiber beam splitter, C1 and C2 are collimators.

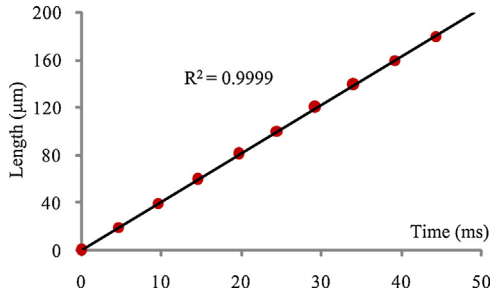

Fig. 5. Best-fit line of time and length scale.

The laser beam crosses an optical fiber circulator (CIR) to the fiber beam splitter (FBS), and then the beam is divided into two paths by the FBS. One beam falls onto a scanning mirror (M1) that is fixed on a voice coil actuator; the other falls onto a target mirror (M2) attached to a precise translation stage via a collimator (C2) and a sapphire window (SW). A linear gauge (Laser Hologauge LGH-110, Mitutoyo) with a resolution of 10 nm was installed behind a target mirror (M2). In practice, two interference fringes will occur on the screen of an oscilloscope when the distance from the reference position to the target is approximately 150 mm. After that, the target was moved far away from the reference position by a translation stage controller (FC-401, Sigma Tech). Then, the length scales were measured by a linear gauge. Using the same process, the time scales were determined from the peak-to-peak measurement of the envelope interference fringes, which appeared on the screen of an oscilloscope. In this experiment, a voice coil actuator was operated with a constant speed of 0.001 m/s. The measurement results are shown in Fig. 5.

Fig. 5 is a least-squares fitting of the data set between the length scale (y-axis) and the time scale (x-axis); this was repeated 11 times. The maximum deviation between the dependent variable (length scale) and the best-fit line is approximately 0.31 μm, the standard deviation is approximately 0.23 μm, and the correlation coefficient (R^2) is approximately 0.9999. This indicates that two data sets match a straight line that is obtained by a correlation coefficient value. This relation is linear. In experiments, the hysteresis of the scanning-fringe device is not considered because a one-way direction of scanning fringe is required for the proposed method. Conversely, this relation relates to the scanning speed of a voice coil actuator. Therefore, a constant speed of the scanning-fringe device is necessary during measurement.

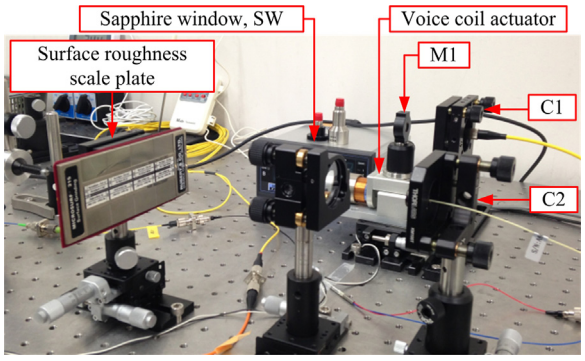

Fig. 6. Measurement setup to determine the effect of the surface roughness of targets on interference fringes.

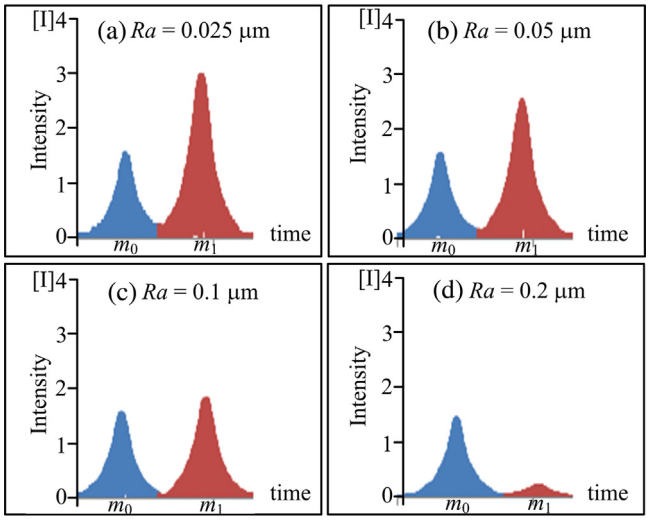

Fig. 7. Intensity of the interference fringes on different target *Ra* values; the red graphs are the fringes which come from the target, others come from the reference position. (For interpretation of references to colour in this figure legend, the reader is referred to the web version of this article.)

3.2. Surface roughness of the target

This experiment explains the effect of the surface roughness of the target on the absolute length measurement. The measurement setup is illustrated in Fig. 6.

A surface roughness scale plate with *Ra* values of 0.025 μm, 0.05 μm, 0.1 μm, and 0.2 μm was used as the target 150 mm from the reference position. Then, the interference fringes were recorded. The results are shown in Fig. 7

The results in Fig. 7 indicate that the intensity of the interference fringes, which are reflected from the surface of the target, is significantly weak if the value of *Ra* is increased. Next, the same plate was moved to a distance of 1500 mm. The length from the reference position to the targets was measured 10 times and evaluated by Eq. (2). The measured standard deviations of length were obtained and paired with the roughness surface of the target. The experimental results are shown in Table 1.

The standard deviations of the length measurement are shown in Table 1; they are gradually enlarged if the value of *Ra* value of the target is increased. When the surface roughness of the target is greater than 0.2 μm, it cannot be used as the target because the reflected beam from that target is not returned to single-mode fiber of the interferometer. The results from both Fig. 7 and Table 2 indicate that the surface roughness of the target significantly affects the performance of the proposed measuring system.

Table 1
Standard deviations of length measurement to surface roughness targets.

Nominal length (mm)	Surface roughness, *Ra* (μm)	Standard deviations (μm)
1500	0.025	0.59
	0.05	0.64
	0.1	0.74
	0.2	–

Table 2
Positioning measurement results of *y*-axis of a CMM.

CMM (mm)	Proposed method (mm)	Position error 1 (μm)	Standard deviation (μm)
0.000	0.0000	0.00	0.00
149.857	149.8557	1.31	0.29
299.714	299.7127	1.33	0.41
449.571	449.5690	2.01	0.47

CMM (mm)	Renishaw laser (mm)	Position error 2 (μm)	Standard deviation (μm)
0.000	0.0000	0.00	0.00
149.857	149.8559	1.11	0.14
299.714	299.7126	1.43	0.21
449.571	449.5692	1.77	0.24

3.3. *The measurement of positioning accuracy of a CMM*

In this experiment, a rough metal ball was used as the target of a single-mode fiber interferometer for the positioning measurement of a CMM. A single-mode optical fiber more than 100 m long was used to connect a laser source from the 10th floor of a building to the proposed measuring system inside a CMM room in the basement of the building. Then, the positioning accuracy of a CMM was measured and paired with a cw laser interferometer (Renishaw). The measurement setup is shown in Fig. 8.

A rough metal ball with an *Ra* of 0.1 μm; a diameter of 25 mm and a retroreflector were attached to the probing system of a CMM. A moving bridge-type CMM (FALCIO APEX 707, Mitutoyo) was used in this experiment. The positions of measurement were controlled by the CMM controller. Then, the linear positions of a CMM were measured by the Renishaw laser interferometer and the proposed measuring system. This experiment was conducted in an environmental control room. The average air temperature, relative humidity and air pressure were approximately 22.35 °C, 21.1%RH, and 100.40 kPa, respectively. The measurement results of five time repetitions are summarized in Table 2.

The measurement results shown in Table 2 were corrected for the group refractive index of air to the reference temperature [19]. The position error 1 shows the position errors of a CMM that are determined by the difference between the values of the CMM positions and the values measured by the proposed method. The position error 2 is determined by the difference between the values of the CMM positions and the values measured by the Renishaw laser interferometer. The maximum standard deviation of the measurement is approximately 0.47 μm for the proposed measuring system and 0.24 μm for the Ranishaw laser interferometer. The graph in Fig. 9 shows the position errors of the *y*-axis of a CMM paired with the maximum permissible error of indication of a CMM for size measurement—$[MPE_E = \pm(1.9 + 3L/1000)]$ μm, where L is the indication length of a CMM in mm. This indicates that the position errors of a CMM show the same trends when measured by both measuring systems. The maximum difference between two curves is approximately 0.24 μm. These results suggest that the proposed measuring system can be applied successfully with high accuracy for industrial CMMs. However, the maximum permissible error of a CMM includes usage of a contact probing system when the measurement is performed. On the other hand, the proposed measuring system is a non-contact type of measurement, and does not contain the effect of the probing error.

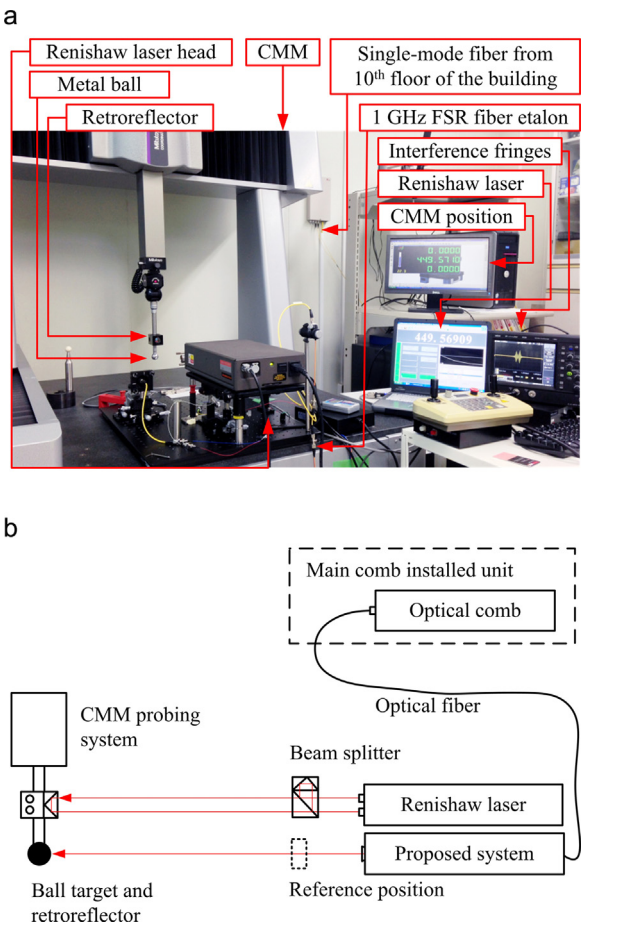

Fig. 8. CMM positioning measurement using proposed measuring system paired with Renishaw laser interferometer. (a) The photograph of measurement. (b) The measurement setup diagram.

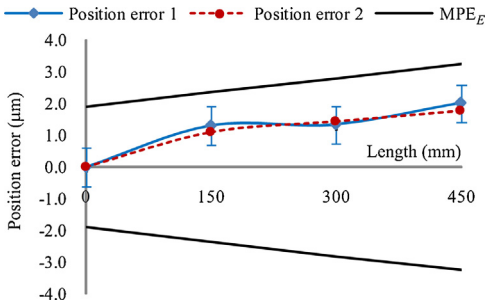

Fig. 9. Position errors of *y*-axis of a CMM; the blue solid line is the position errors of a CMM with gap of the measurement uncertainty that were measured by proposed system. The red dash line is the position errors of a CMM that measured by Renishaw laser interferometer, and the black lines are the maximum permissible error of indication of a CMM for size measurement. (For interpretation of references to colour in this figure legend, the reader is referred to the web version of this article.)

4. Uncertainty of measurement

The uncertainty of CMM positioning measurements has been evaluated following the recommended guideline [20]. The sources of errors under consideration may be divided into three groups. The first group involves the modified frequency source of the optical comb by the Fabry–Pérot fiber etalon. The stability of the

Table 3
Uncertainty evaluation of CMM positioning measurement.

Uncertainty source	Uncertainty value	Uncertainty contribution
Stability of modified frequency source	$<1 \times 10^{-9}$	$2.89 \times 10^{-1}L$
Refractive index of air	1.43×10^{-7}	$1.43 \times 10^{-7}L$
Air temperature	0.15 K	
Air pressure	0.64 kPa	
Air humidity	0.25%RH	
Cidder's formula	2.1×10^{-8}	
Thermal expansion	1×10^{-6}	$8.66 \times 10^{-8}L$
Repeatability of measurement	0.21 μm	
Time and length scale measurement	0.18 μm	
Combined standard uncertainty ($k=2$)	$[(0.56)^2 + (33.4 \times 10^{-3}L)^2]^{1/2}$ μm	

Note: L is the indication length of a CMM in mm.

repetition frequency after passing a Fabry–Pérot fiber etalon is in the order of 10^{-9} over 2 h. This cause is a partial contribution of $0.5 \times 10^{-9}L$ divided by the rectangular distribution, because of semi-range limits of a finite resolution of the used instrument. The uncertainty of the repetition rate and carrier offset frequency is canceled because the accuracy ratio with the MPE_E of a CMM is more than 100 times better. The second group includes the environmental conditions, the compensation of the group refractive index of air, and thermal expansion of linear scale of a CMM. Because of the measurement errors of environmental conditions (air temperature, air pressure and, air humidity) during measurement, the contribution uncertainty of each parameter were determined by the standard uncertainty of each parameter multiple by their sensitivity coefficients. Therefore, the compensation uncertainty for the refractive index of air was calculated to be $1.43 \times 10^{-7}L$, where L is the indication length of a CMM. It was a root of square-sum of distribution uncertainties of air temperature, air pressure, air humidity and Cidder's formula. The coefficient of thermal expansion of the linear scale of a CMM is approximately of 8.0 μm m^{-1} K^{-1} with an uncertainty of ± 1 μm m^{-1} K^{-1}. In this experiment, the changes of temperature of linear scale of a CMM cannot be measured directly. Therefore, the uncertainty due to thermal expansion of linear scale in a CMM was determined from the changes of air temperature, because thermal expansion effect of a CMM was compensated automatically to reference temperature (20 °C) by CMM's software and the measurement values of the air temperature are generally utilized in the place of the scale temperature.

The last group involves the measurement procedures such as measurement repeatability and the uncertainty of time and length scale measurement. The uncertainty of measurement repeatability was approximately 0.21 μm which was evaluated from the maximum standard deviation of five times of measurement repetitions. The uncertainty due to the relationship of time and length measurement is evaluated from the maximum deviation between the measured values and the best-fit line and it was assumed to be a rectangular distribution. The error sources and their uncertainties of the measurement uncertainty are summarized in Table 3.

5. Conclusions

An optical-comb pulsed interferometer whose repetition frequency is transferred from 100 MHz to 1 GHz by an optical fiber-type Fabry–Pérot etalon was developed to verify the positioning measurements of industrial CMMs. A rough metal ball with an *Ra* of 0.1 μm was used as a target of the single-mode fiber interferometer. A moving bridge-type CMM was measured by the proposed technique paired with a Renishaw laser interferometer in an environmental control room. Both systems show the same trend of position error. The expanded uncertainty of positioning measurement is approximately 0.6 μm at the length of 450 mm. The results show that the measurement accuracy is mainly affected by changes in the environmental conditions, while the noise of the interference fringe is caused by air fluctuation and mechanical vibration. The proposed measurement technique is very convenient and is easier to align than using end standards or a continuous-wave laser interferometer. It also provides enough accuracy for measuring linear dimensions of industrial CMMs. The proposed measuring system can be installed at any location on the surface of a CMM. It can also be used on more than one system to measure the lengths because a rough sphere ball offers a 3D target for a single-mode fiber interferometer. Therefore, further research will be undertaken in the future to study the volumetric errors of CMMs.

References

[1] ISO10360-1. Geometrical Product Specification (SPC). Acceptance and reverification tests for coordinate measuring machines (CMM). Part 1: Vocabulary. International Organization for Standardization; 2000.
[2] Barakat NA, Elbestawi MA, Spence AD. Kinematic and geometric error compensation of a coordinate measuring machine. Int J Mach Tool Manuf 2000;40:833–50.
[3] ISO10360-2. Geometrical Product Specification (SPC). Acceptance and reverification tests for coordinate measuring machines (CMM). Part 2: CMMs used for measuring linear dimensions. International Organization for Standardization; 2009.
[4] EAL-G17. Coordinate measuring machine calibration. European Cooperation for Accreditation of Laboratories; 1995.
[5] Aguilar JJ, Aguado S, Santolaria, Samper D. Mutilateration in volumetric verification of machine tool. In: XX IMEKO World Congress. 2012.
[6] Schwenke H, Schmitt R, Jatzkowski P, Warmann C. On-the-fly calibration of linear and rotary axes of machine toolts and CMMs using tracking interferometer. CIRP Ann Manuf 2009;58:477–80.
[7] Trapet E, Wäldele F. A reference object based method to determine the parametric error component of coordinate measuring machines and machine tools. Measurement 1991;9:17–22.
[8] Swornowski PJ. A new concept of continuous measurement and error correction in Coordinate Measuring Technique using a PC. Measurement 2014;50:99–105.
[9] Weckenmann A, Lorz J. Monitoring coordinate measuring machine by calibrated parts, 7th International Symposium on Measurement Technology and Intelligent Instruments. J Phys: Conf Ser 2005;13:183–90.
[10] Curran E, Phelen P. Quick check error verification of coordinate measuring machines. J Mater Process Technol 2004;155–156:1207–13.
[11] Abbe M, Takamasu K, Ozono S. Reliability on calibration of CMM. Measurement 2003;33:359–68.
[12] Cauchick-Miguel P, King T, Davis J. CMM verification: a survey. Measurement 1996;17:1–16.
[13] Cundiff ST, Ye J. Femtosecond optical frequency comb. Rev Mod Phys 2003;75:325.
[14] Wang X, Takahashi S, Takamasu K, Matsumoto H. Spatial positioning measurements up to 150 m using temporal coherence of optical frequency comb. Precis Eng 2013;37:635–9.
[15] Matsumoto H, Wang X, Takamasu K, Aoto T. Absolute measurement of baselines up to 403 m using heterodyne temporal coherence interferometer with optical frequency comb. Appl Phys Express 2012;5:046601.
[16] Chanthawong N, Takahashi S, Takamasu K, Matsumoto H. Performance evaluation of a coordinate measuring machine's axis using a high-frequency repetition mode of a mode-locked fiber laser. Int J Precis Eng Manuf 2014;15:1507–12.
[17] Balling P, Křen P, Mašika P, van den Berg SA. Femtosecond frequency comb based distance measurement in air. Opt Express 2009;17:9300–13.
[18] Ciddor PE, Hill RJ. Refractive index of air. 2. Group index. Appl Opt 1999;38:1663–7.
[19] ISO 1. Geometrical product specification (SPC). Standard reference temperature for geometrical product specification and verification. International Organization for Standardization; 2002.
[20] EA-4/02. Evaluation of the uncertainty of measurement in calibration. European Co-operation for Accreditation; 2013.